Chemical Engineering and Processing 71 (2013) 97–106

Chemical Engineering and Processing: Process Intensification

journal homepage: www.elsevier.com/locate/cep

An evaluation of the effectiveness of continuous thin film processing in a spinning disc reactor for bulk free-radical photo-copolymerisation

Christopher G. Dobie [1], MarijaVicevic [2], Kamelia V.K. Boodhoo *

School of Chemical Engineering and Advanced Materials, Newcastle University, Newcastle Upon Tyne NE1 7RU, United Kingdom

ARTICLE INFO

Article history:
Received 9 November 2012
Received in revised form 2 February 2013
Accepted 8 March 2013
Available online 28 March 2013

Keywords:
Process intensification
Spinning disc reactor
Free-radical photo-copolymerisation
Vinyl acetate
Butyl acrylate
Thin films

ABSTRACT

This paper reports on UV-initiated free-radical copolymerisation of vinyl acetate with *n*-butyl acrylate (VAc-BA) under conditions of thin film flow in a spinning disc reactor (SDR). Almost 40% overall monomer conversion can be achieved in under 5 s under optimised operating conditions in the SDR, with controlled molecular weight properties of the copolymer, highlighting the good levels of mixing in the film. Residence time on the SDR is a limiting factor in the extent of conversion achievable in a single pass. Comparison with a static film demonstrates the superiority of the SDR in maintaining a high overall rate of polymerisation. Composition of the copolymer formed in the SDR indicates that, due to its plug flow behaviour, the SDR cannot address the inherent problem of compositional drift.

We have shown that efficiency of light absorption is dictated by conditions favouring longest UV exposure times, rather than thinner films on the disc. Initiator decomposition efficiency, an important consideration in the overall rate of the co-polymerisation, is enhanced by lower fluid flowrates. This study highlights the promising technology offered by the SDR in combination with UV irradiation for the exploitation of photo-copolymerisation as a viable method for bulk copolymer synthesis.

1. Introduction

Copolymerisation is a powerful method for introducing systematic changes in polymer properties. It is hugely important from a commercial standpoint. The ability to incorporate into the same polymer molecule, in varying proportions, monomer units having diverse physical and/or chemical properties allows for enormous flexibility in the manufacture of copolymers with narrowly defined properties. For example, the vinyl acetate–butyl acrylate (VAc–BA) copolymer finds application as an architectural coating, sealant and adhesive [1,2].

The bulk method of copolymerisation is a potentially environmentally friendly processing route. Avoiding the use of additives such as solvents, surfactants or suspension stabilisers means that less downstream processing is required, thereby saving money and energy. Obviously, the disposal or storage of these potentially environmentally harmful materials upon purification of the final polymer product becomes less of an issue. It also means that the yield of product per volume of reactor is greater than for other common production techniques such as emulsion polymerisation. However, in spite of the described advantages of the bulk polymerisation process, only few polymers such as polyethylene and poly(methyl methacrylate) [3] and high-impact polystyrene [4] are manufactured using this method, usually in a number of stages and in specialised tower reactors at high conversions [3,4]. This method of polymerisation is therefore generally unsound for producing high quality, high conversion polymers in conventionally employed large stirred tank reactors which suffer from limited heat transfer and mixing capacities, more so in the presence of highly viscous reaction media.

The emergence of UV radiation as an inexpensive and efficient alternative technique of initiating polymerisation has benefited numerous processes such as industrial cross-linking processes, curing applications such as dental restorations, optoelectronics and adhesive manufacturing [3] as well as surface grafting reactions in order to modify polymer surfaces [5,6]. Moreover, a large number of investigative kinetic studies are performed using photoinitiators since the start and end times of initiation and, thus, polymerisation, can be exactly defined [7]. UV radiation has the potential to introduce numerous savings resulting from the high reaction rates obtainable coupled with reduced energy requirements [8]. It is a rapid process that can be controlled much more effectively than thermal initiation by simple variation of the incident radiation intensity [3]. Furthermore, the fact that photo-initiation can take place over a wide temperature range provides a greater degree of tacticity control of the polymer product [3,9]. There is also

* Corresponding author. Tel.: +44 191 222 7264.
E-mail address: kamelia.boodhoo@ncl.ac.uk (K.V.K. Boodhoo).
[1] Present address: Johnson Matthey, Billingham, Cleveland TS23 1LB, United Kingdom.
[2] Present address: Faculty of Technical Sciences, Department of Energy and Process Engineering, Trg Dositeja Obradovica 6, Novi Sad, Serbia.

0255-2701 © 2013 Elsevier B.V. Open access under CC BY-NC-ND license.
http://dx.doi.org/10.1016/j.cep.2013.03.011

Nomenclature

A_{disc}	surface area of rotating disc (m^2)
c	speed of light ($m\,s^{-1}$)
$C, \bar{C}$	concentration of light absorbing species ($mol\,L^{-1}$)
f	frequency of UV radiation (s^{-1})
F_i	mole fraction of monomer i in the copolymer
h	Planck's constant (J s)
I	intensity of transmitted light (mW/cm^2)
I_0	incident light intensity (mW/cm^2 or mol photons $10^{-3}\,cm^{-2}\,s^{-1}$)
$\bar{I}_a$	average absorbed light intensity across the film thickness (mol photons $10^{-3}\,cm^{-2}\,s^{-1}$)
$I_{a,disc}$	light energy absorbed over whole disc area in one disc pass (mol photons)
K	consistency index ($Pa\,s^n$)
l	film thickness (cm)
M_{DMPA}	molecular mass of DMPA ($g\,mol^{-1}$)
M_n	number average molecular weight ($g\,mol^{-1}$)
n	flow behaviour index
N_A	Avogadro's number (mol^{-1})
n_i, n_j	number of moles of components i, j, in the feed mixture
$[PI]_0$	initial initiator concentration (% w/w)
$[PI]_{disc}$	amount of initiator present on disc surface (mol)
Q	feed flowrate ($m^3\,s^{-1}$)
r	radial distance from centre of disc (m)
R_p	polymerisation rate ($mol\,L^{-1}\,s^{-1}$)
t	time (s)
t_{res}	mean residence time on rotating disc (s)
V_r	film radial velocity ($m\,s^{-1}$)
x	individual monomer conversion (%)
X	overall conversion to copolymer (%)
z	vertical distance from disc surface (m)

Greek symbols

α	absorption coefficient ($L\,mol^{-1}\,cm^{-1}$)
$\dot{\gamma}(r,z)$	shear rate at radial position r and vertical distance z (s^{-1})
φ	quantum yield of initiation (assumed to be 0.6 [35])
λ	incident light wavelength (m)
μ_a	apparent viscosity (Pa s)
ν	kinematic viscosity of polymerising film ($m^2\,s^{-1}$)
ρ	density ($g\,L^{-1}$)
ω	angular velocity on rotating disc ($rad\,s^{-1}$)

Abbreviations

BA	butyl acrylate
DMPA	2-2-dimethoxyphenylacetophenone
MEHQ	4-methoxyphenol
VAc	vinyl acetate

the added benefit that temperature changes may be implemented without adversely affecting the initiation step. This option of decoupling the effects of temperature on the initiation and propagation rates is not available in a thermally initiated system. Because thermal initiators often have a temperature range within which they work optimally, the operating temperature has to be selected primarily on that basis and may not be the ideal temperature for the overall polymerisation process.

The main challenges with employing this method of initiation in conventional stirred tank polymerisers are related to UV penetration into the polymerising mixture, which is governed by the optical properties of the absorbing material and by its concentration according to the Beer–Lambert law. UV penetration depths can be significantly limited to a few millimetres into the mixture especially at high concentrations of the absorbing species [10]. This may result in inefficient use of the large reactor volumes typically employed in commercial scale stirred tank reactors unless adequate stirring is provided to allow constant recirculation of the fresh absorbing species near the UV source [11]. The immersion-well batch reactor [11] commonly used for photochemical processes is based on these principles. One potential problem in such reactors is that unusually long processing times may be required, more so in viscous media, for photochemical reactions to reach completion due to the additional recirculation times. Improved designs of photochemical reactors, where the efficiency of light absorption is enhanced mainly through thin film formation, have been suggested and they include falling-film reactors where a thin film flows down surfaces of various configurations under gravity [12,13] and continuous flow microreactors [10]. However, limited information is available in the literature on applications of these improved versions of photo-reactors for bulk homo- or co-polymerisation processes [14] which are renowned for the challenges involved in their handling due to their typically high viscosities.

The spinning disc reactor is a continuous flow reactor technology which offers significant benefits for the exploitation of photopolymerisation using the bulk procedure. Not only does the centrifugal force enable relatively easy flow of viscous polymer mixtures but the viscosities can also be reduced under the high shear rates in the film. Moreover, the efficiency of UV-initiation can be enhanced via extremely efficient penetration of the thin films generated on the disc surface. The ability to vary the thickness of the film by controlling the disc rotational speed is a bonus feature which is not available in the falling film reactors operating under gravity. Past studies on the SDR [15] have demonstrated that significant levels of conversion (>90%) can be attained for fast bulk *homo*polymerisations (*n*-butyl acrylate) employing UV radiation as a means of initiating the reaction. More recently, a study involving UV-induced graft copolymerisation of acrylic acid and vinyl-oxybutyl-polyethylene glycol in the SDR has reported 70% conversion of acrylic acid in 2 passes on a 20 cm diameter disc [16]. Additionally, molecular weight distributions (MWDs) have been observed to be narrow, even at high conversion, suggesting that the excellent mixing reduces or eliminates the gel effect typically observed in conventional high-viscosity polymerisation processes [15,16]. In this present contribution, we address photo-induced bulk co-polymerisation in the SDR, on which no work has been reported to date. The unique challenges in controlling the formation and properties of co-polymers in general make this study all the more worthwhile.

2. Experimental work

The performance of a spinning disc reactor (SDR) for the bulk free-radical photo-copolymerisation of vinyl acetate with butyl acrylate at 75 °C (348 K) was studied and compared with a static film process. With this comparison, our objective was to investigate the effect of film mixing on the copolymerisation rate and the copolymer properties. The choice of monomers used was influenced by two major factors. Primarily, the rate constant for propagation of this co-monomer system is relatively high – approximately 17,060 $L\,mol^{-1}\,s^{-1}$ at 348 K [17] – so that polymerisation should still be able to occur even during the short residence times offered on the SDR. Secondly, there is a large difference between the reactivity ratios of these two monomers ($r_{BA} = 5.93$ and $r_{VAc} = 0.026$), such that any improvement in copolymer homogeneity as compared to the static film system should be much

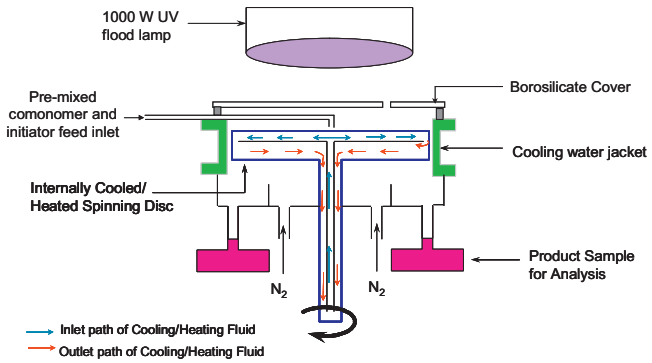

Fig. 1. Schematic of the SDR.

more apparent than if a system having similar reactivity ratios such as, for example, styrene and methyl methacrylate ($r_S = 0.55$ and $r_{MMA} = 0.49$), were to be used. The initiator used was 2,2-dimeth-2-phenyl oxyacetophenone (DMPA) (Aldrich) and free-radicals were generated through UV irradiation of 366 nm wavelength.

2.1. Materials

n-Butyl acrylate (BA) and vinyl acetate (VAc) (Aldrich) were washed of inhibitor by filtration through an alumina column, refrigerated in a dark bottle and used within one month of purification. 2,2-Dimethoxy-2-phenyl acetophenone (DMPA) initiator and tetrahydrofuran (THF) (Aldrich) were used as received. 4-Methoxyphenol (MEHQ) in toluene (Aldrich) was used to quench the polymerisation. Oxygen-free nitrogen was used as received from BOC gases.

2.2. Spinning disc reactor (SDR)

The SDR, shown schematically in Fig. 1, consists of a 150 mm diameter stainless steel disc. A stainless steel feed pipe of 3 mm in diameter is introduced from the side of the reactor and runs across the disc to deliver the pre-mixed co-monomer and initiator feed onto the centre of the disc. A borosilicate cover also allows for a contained environment within which an inert atmosphere may be maintained as well as allowing for efficient penetration of the desired UV wavelength (366 nm). The other standard features of the SDR set-up have been described in an earlier publication [18].

2.3. SDR experimental procedure

Purified VAc and BA were weighed and mixed to produce an 85:15 wt% mixture, respectively. The desired quantity of photoinitiator was stirred into the co-monomer mixture until completely dissolved. The reaction mixture was sparged with nitrogen using a sintered glass distributor for 15 min to de-oxygenate the mixture. The flow of water from the temperature-controlled bath through to the underside of the disc surface was started, with the disc temperature controlled at 348 K. The UV lamp (1000 W mercury lamp, UV light Technology Ltd., having an emission peak at wavelength 366 nm – the absorption wavelength of DMPA) was switched on and allowed to warm up for 15 min. UV intensity was varied by adjusting the distance of the lamp from the disc surface in accordance with a calibration performed before experimentation using a hand-held sensor (UV Technology Ltd.) positioned at different distances from the lamp. This calibration procedure was repeated periodically to ensure the calibration remained valid throughout the course of the experimentation with the lamp. Prior to feeding the monomers/initiator mixture onto the disc surface, the reactor was purged with nitrogen for at least 20 min. During this time, the disc rotation was started at the desired speed. A sample of the co-monomer/initiator mixture was taken prior to feeding to the SDR. The mixture was introduced onto the disc at the desired flow rate using a calibrated peristaltic pump connected to a pulse dampener to allow a smooth continuous flow of the feed mixture. Samples of the SDR product were then collected from the SDR product outlet tubes. To ensure representative samples, three drops of the MEHQ solution were immediately added to the samples in order to prevent further copolymerisation prior to analysis.

Table 1
Operating parameters studied in SDR.

Operating parameter	Parametric values
Disc rotational speed, N (rpm)	160, 180, 210
Feed flowrate, Q (ml/s)[a]	0.625, 1.25
Incident UV intensity, I_o (mW/cm^2)	33, 60, 106
Initial photoinitiator concentration, $[PI]_0$ (% w/w of monomer)	2, 3.5, 5

[a] Flowrate was not included in the full factorial design of experiment which was conducted at constant flowrate of 1.25 ml/s. Limited experiments were performed at the lower flowrate.

Randomised general full factorial experimental designs based on the disc speed, UV intensity and photo-initiator concentration, the ranges for which are indicated in Table 1, were created in Minitab.

2.4. Static film apparatus

The static film cell consisted of a stainless steel block in which a circular well was machined (Fig. 2). A hole of 1 cm in diameter was drilled in the base of the well to accommodate the FTIR probe for online monitoring of the polymerisation reaction. The test cell also had a provision for cooling water to be recirculated through its base. A thermocouple protruding through the film at the base of the well recorded the film temperature. A nitrogen purge was introduced through an inlet in the cell wall and exited through an outlet port on the opposite wall, enabling an oxygen-free atmosphere to be maintained in the cell. A removable borosilicate cover was secured in place on the top surface of the cell.

2.5. Static film experimental procedure

The procedure for preparing the co-monomer/initiator mixture was as described for the SDR experiments. The operating temperature of 348 K was maintained by water from the temperature-controlled bath. The static film test cell was purged with nitrogen for at least 15 min in order to deplete oxygen levels in the cell atmosphere. The volume of co-monomer/initiator mixture needed to generate the required film thickness was then injected via a syringe through the silicon rubber sealable port into the central well of the cell. At this point, a time, $t = 0$ spectrum was captured using the FTIR software (ReactIR 2000, Mettler Toledo). The UV lamp was placed above the static film cell at a set distance. A second FTIR spectrum was captured at specified reaction times which ranged between 5 and 30 s. Several drops of MEHQ solution were added to quench the reaction and the product was dissolved in THF and further prepared for molecular weight analysis using gel permeation chromatography (GPC).

2.6. Characterisation

The characteristics of interest in this study were overall monomer conversion, copolymer composition and molecular weight properties, in particular M_n and polydispersity index (PDI).

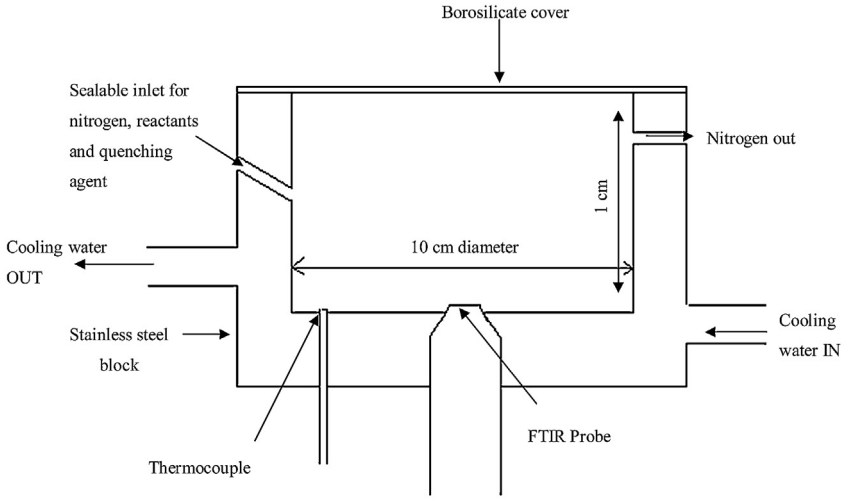

Fig. 2. Schematic of the static film cell.

Overall conversion of monomers to copolymer and copolymer composition were analysed via FTIR spectroscopy (ReactIR, Mettler Toledo). SDR measurements were carried out off-line using samples collected from the product outlet whilst real-time online measurements were obtained in the static film test cells. Characteristic absorbance peaks at 810 cm^{-1} for BA and 1290 cm^{-1} for VAc were found in the literature [2]. Conversion (x) of each individual monomer and the overall conversion X at time t were estimated from Eqs. (1) and (2) respectively, following the procedure described in [2]. The instantaneous copolymer composition at time t can then be determined (Eq. (3)).

$$x \ (\text{mol\%}) = 1 - \frac{\text{peak height at } t}{\text{peak height at } t = 0} \times 100 \quad (1)$$

$$X \ (\text{mol\%}) = \frac{n_1}{n_1 + n_2} x_1 \ (\text{mol\%}) + \frac{n_2}{n_1 + n_2} x_2 \ (\text{mol\%}) \quad (2)$$

$$F_i = \frac{n_i x_i}{n_i x_i + n_j x_j} \quad (3)$$

Molecular weight M_n and PDI of the copolymer were determined by GPC with two PL gel 5 μm Mixed-C columns (Polymer Laboratories) using tetrahydrofuran (THF) as the eluent flowing at a rate of 1 ml min^{-1} through the column at 30 °C. Samples for analysis were prepared by weighing approximately 100 mg of the sample and making up to 10 ml with THF. A single drop of styrene monomer was added to the prepared samples to correct for flow rate fluctuations. Molecular weight characterisation was carried out against polystyrene calibration standards supplied by Polymer Laboratories.

Experimental errors in overall monomer conversion, molecular weights and PDI, determined by repeating various randomly selected experiments, were estimated generally to be no more than 10%. The source of the greatest errors for the overall monomer conversions was collection of a representative sample from the outlet port of the SDR, which was made more difficult as the viscosity of the sample increased. For M_n and PDI, the manual identification of the copolymer peaks would have contributed significantly to the errors observed in the GPC measurements.

3. Results and discussion

The free-radical copolymerisation process proceeds via a three step mechanism involving initiation, propagation and termination

$$I \xrightarrow{hf} R_1^* + R_2^*$$

$$R^* + X \longrightarrow RX^* \text{ (where X = monomer 1 or 2)}$$

Scheme 1. Initiation steps.

$$RX_n^* + M_1 \longrightarrow RX_nM_1^*$$

$$RX_n^* + M_2 \longrightarrow RX_nM_2^*$$

Scheme 2. Propagation steps.

$$\text{Termination by combination: } RX_n^* + {}^*X_mR \longrightarrow RX_{n+m}R$$

$$\text{Termination by disproportionation: } RX_n^* + {}^*X_mR \longrightarrow RX_p + RX_q$$

Scheme 3. Termination steps.

(assuming negligible chain transfer) as depicted in Schemes 1–3 below [3]:

3.1. SDR experiments

The main effects plots showing the influences of disc speed, initial photo-initiator concentration $[PI]_0$ and incident UV intensity I_o on overall monomer conversion and on M_n are displayed in Figs. 3 and 4. The p-values for each of these parameters are very small, indicating the significant effect of each on the measured values.

3.1.1. Effect of disc speed and feed flowrate

Variations in the disc speed and feed flowrates have profound effects not only on residence time on the rotating disc surface (t_{res}), but also on film thickness (l) which are determined from Eqs. (4) and (5) [18]. Higher disc speeds reduce both the residence time and film thickness whereas higher feed flowrate causes an increase in the film thickness and a decrease in the residence time.

$$t_{res} = \left[\frac{81\pi^2\upsilon}{16\omega^2Q^2}\right]^{1/3} (r_0^{4/3} - r_i^{4/3}) \quad (4)$$

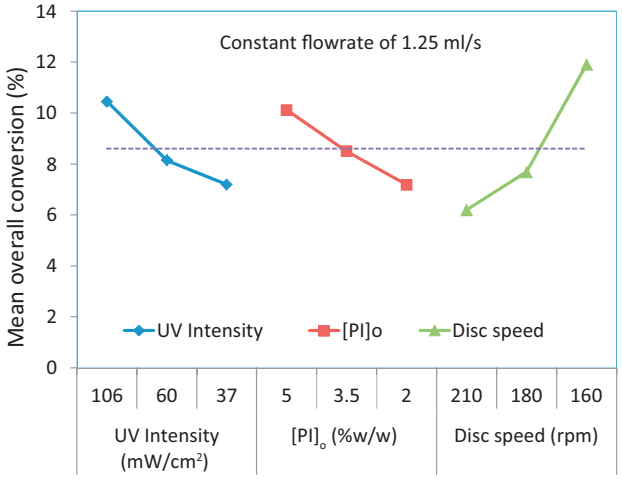

Fig. 3. Main effects plots for overall monomer conversion in SDR.

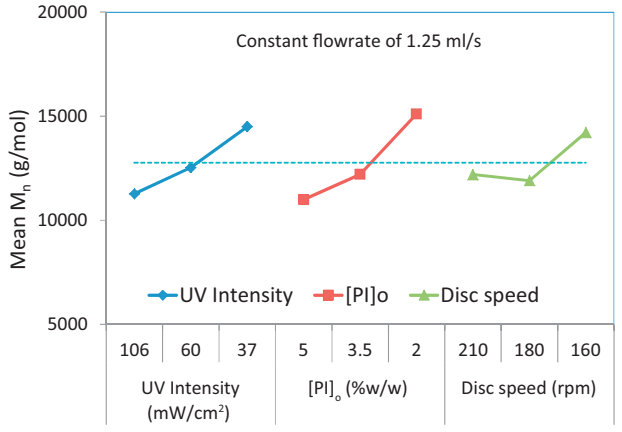

Fig. 4. Main effects plots for M_n of polymer formed in SDR.

$$l = \left[\frac{3\nu Q}{2\pi\omega^2 r^2}\right]^{1/3} \quad (5)$$

From Fig. 3, it is observed that monomer conversion increases with a decrease in disc speed. This trend highlights the greater dependence of monomer conversion upon residence time rather than film thickness since with decreasing disc speed (analogous with increasing residence time) the conversion increases, in spite of the increasing film thickness. It is very reasonable to expect that, given a longer time within which to react, more copolymerisation would take place. From Eq. (4), disc residence time is observed to be dependent on several factors other than disc speed (represented by ω, where $\omega = 2\pi N/60$), such as flowrate Q, and disc radius, r_o. Therefore changes in the latter two variables are also expected to influence the progress of the reaction in one disc pass. This is indeed reflected in Fig. 5a where a 50% decrease in the original flowrate at constant disc speed of 160 rpm (corresponding to an increase in disc residence time from 2.2 to 3.4 s) is seen to more than double the overall conversion to 37% at the highest initiator concentration. This conversion represents the highest conversion achieved from the SDR experiments reported in this work using a relatively modest disc size of 15 cm diameter.

Molecular weights show a general tendency to be reduced with increasing disc speed (Fig. 4) and decreasing flowrate (Fig. 5b). A similar effect was observed in the photo-polymerisation of *n*-butyl acrylate to produce homopolymers in the SDR [15]. We attribute the observed decrease in M_n with disc speed to the greater centrifugal force acting on the thinner films formed at higher disc speed, as a

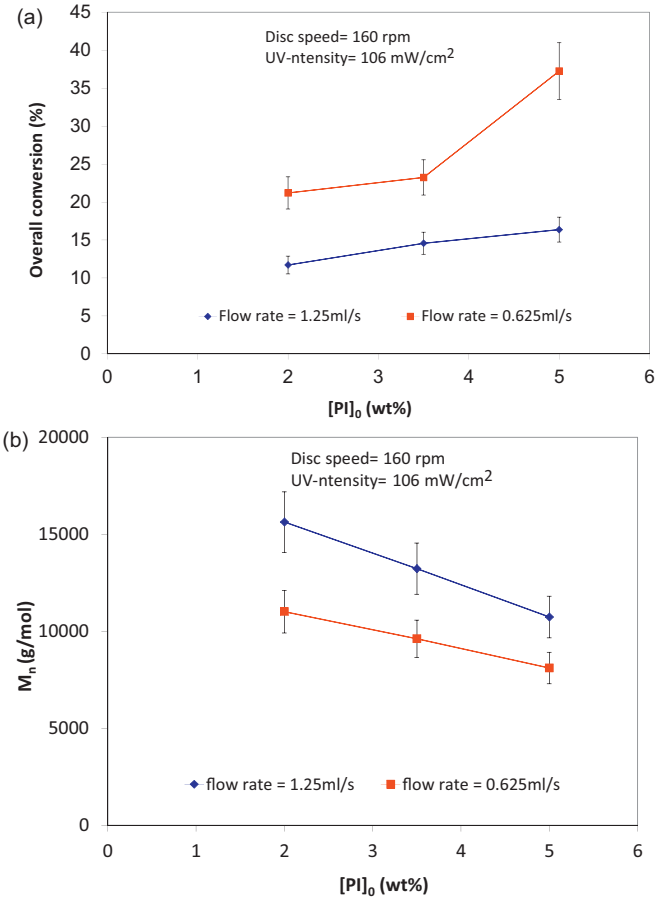

Fig. 5. Effect of SDR feed flowrate on (a) overall conversion and (b) M_n.

result of which shear rate in the film will be higher. This increased shear rate can give rise to two possible effects in the film. Firstly, shear deformation of the polymer molecules will result in a reduction in the viscosity of the film, the extent of which is dependent on the shear rate applied to the film and the properties of the polymeric material. This effect is described by the power-law model for shear thinning liquids expressed as in Eq. (6) [19]:

$$\mu_a = K\dot{\gamma}^{n-1} \quad (6)$$

where μ_a is the apparent viscosity (Pa s), K is the consistency index of the polymer system (Pa s^n), $\dot{\gamma}$ is the shear rate (s^{-1}), n is the flow behaviour index, which has a value of between 0 and 1 for shear thinning fluids such as polymer solutions.

Shear rate in the thin film on the disc surface is described by Eq. (7) [20]:

$$\dot{\gamma}(r,z) = \frac{dV_r(r,z)}{dz} = \left(\frac{3Q\omega^4 r}{2\pi\nu^2}\right)^{1/3}\left(1 - \frac{z}{\delta}\right) \quad (7)$$

Within the film, shear rate will be highest next to the disc surface ($z = 0$). Taking this maximum shear rate into consideration, the relationship between the apparent viscosity and the operating parameters Q, ω and r can be derived as:

$$\mu_a \propto (Qr\omega^4)^{\frac{n-1}{2n+1}} \quad (8)$$

Since the value of n is between 0 and 1, the exponent will be negative, implying that the apparent viscosity will decrease as Q, r and ω increase, with the disc speed (represented by ω) having a much greater influence than the other two parameters. Thus, viscosity of the fluid may be significantly lowered at higher disc speeds as it

passes across the disc surface. With this good control of the viscosity even while polymerisation takes place, diffusion limitation problems can be avoided for effective suppression of the gel effect and/or the cage effect.

Secondly, the polymer chains may experience a larger degree of disentanglement in the enhanced shear field on the disc, so that the active free radicals become more strongly orientated away from each other under the centrifugal force. With such an 'ordered' arrangement of polymer chains on the disc and the active ends diverging away from each other, bimolecular termination reactions (shown in Scheme 3) may not take place so readily. Instead, other primary termination reactions with the smaller initiator radicals, which are more mobile in the film and therefore more readily accessible, may become more important. This phenomenon related to the effect of extensional flow in the SDR on the polymerisation system has been elaborated on in an earlier publication [21].

The effect of reduced flowrate on M_n (Fig. 5b) may be explained by a decrease in film thickness and an increase in disc residence time (i.e. a longer film exposure to the incident light), whereby a greater amount of energy is absorbed per unit volume in the lower volume of material passing across the disc surface, resulting in a higher rate of initiator decomposition. Having more active chains and primary radicals in proximity with each other is likely to lead to earlier termination of the active sites by primary radical termination, rather than by bimolecular termination, and thus leading to lower molecular weights.

Molecular weight distribution remains largely unaffected by flow rate and disc speed, with PDI values generally in the range between 1.5 and 1.8, indicating good control of molecular weight distributions under the good mixing conditions achieved on the disc. It is worth mentioning here that the initiation takes place across the whole disc surface due to the whole surface illumination by the flood lamp used in this study. Chains would therefore be initiated across the range of residence times the fluid experiences on the disc, which would tend to form chains with varied molecular weights. Although the MWD is not particularly large in these experiments, presumably because of the rather short UV exposure times (order of seconds), the potential for achieving an even tighter MWD can be envisaged if a point light source of UV or even lasers is employed.

3.1.2. Effect of $[PI]_0$

From Fig. 3, the general trend is for higher conversions to be achieved with an increase in initiator concentration. This is a consequence of more initiator radicals being formed at higher initiator concentration, allowing more polymer chains to be initiated. This promotes an increase in the consumption of the co-monomers, hence, an increase in overall conversion, an effect which is predicted from classical free-radical polymerisation kinetics theory where the rate of polymerisation R_p is known to be proportional to $[PI]_0^{0.5}$ [3,22]. These findings are in contrast to those for the static film experiments where conversion is seen to decrease with initiator concentration (Fig. 6). We attribute the trends in the static films to the so-called spatial variation in the non-mixed films. Thus, an increase in initiator concentration will increase the absorption of light energy and initiation at the top of the film at the expense of the region below, an occurrence which is especially relevant for a non-bleaching photoinitiator such as DMPA as used in this study. This is illustrated in Fig. 7 where the decrease of UV intensity with penetration depth for DMPA is obvious at each of the three initiator concentrations used in this study. Clearly, with increasing penetration depth, the intensity of the light reaching the lower regions decreases quite considerably. Furthermore, this decrease in intensity occurs to a much greater extent when the amounts of non-bleaching initiator species present increase. As the FTIR probe in the present work protrudes through the bottom of the cell, measuring the individual monomer conversions in that lower region, the observed conversion would therefore expected to be significantly reduced in thicker films and at higher initiator concentrations. The lack of mixing in the static films would tend to exacerbate these effects. On the other hand, spatial variations are expected to be significantly minimised in the SDR films in the SDR due to the intense mixing action in the transverse direction [23].

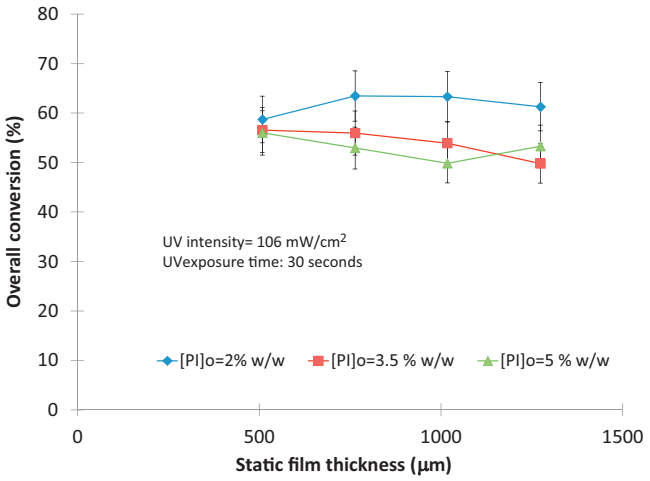

Fig. 6. Effect of initiator concentration on overall conversion in static films.

At higher initiator concentrations in the SDR, more radicals are formed so that earlier termination of the chains by primary radical termination is more likely, thus giving lower molecular weights as seen in Fig. 4. Only a nominal variation of PDI between 1.6 and 1.8 is observed with higher initiator concentration, changes which are within the limits of experimental error.

3.1.3. Effect of UV intensity

Higher levels of energy imparted at higher UV intensities over any given residence time period decompose proportionally more initiator molecules into active radicals. In the presence of a higher number of initiated polymeric chains each of which add a certain number of monomer molecules, there is more monomer consumed overall in one disc pass, leading to the observed increase in conversion, seen in Fig. 3. Molecular weights are shown to decrease with increases in UV intensity, consistent with the fact that more radicals are present, leading to earlier termination and hence lower values

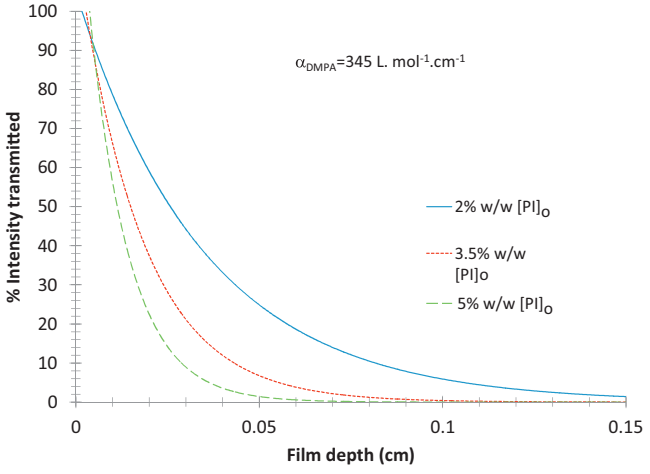

Fig. 7. Variation of light intensity transmission with penetration depth at various concentrations of DPMA photoinitiator.

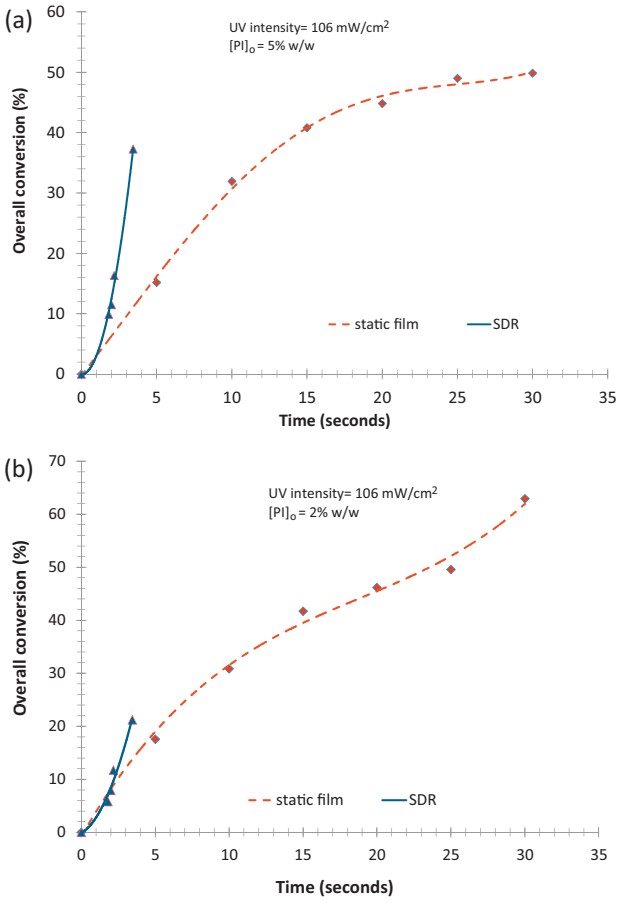

Fig. 8. Conversion in the static film (film thickness = 1018 μm) compared with the SDR using (a) $[PI]_0$ = 5% (w/w), (b) $[PI]_0$ = 2% (w/w).

of M_n (Fig. 4). There is no discernible trend in MWD with changes in the UV intensity, with PDI values remaining consistently within the range 1.6–1.8 at all UV intensities studied.

3.2. Comparison between SDR and static film

3.2.1. Rate of polymerisation

The overall rate of polymerisation, R_p, in the SDR and the static film are compared in Fig. 8a and b. Within the first 5 s of operation in each system, the monomer conversion in the SDR is greater than that in the static film, more so at the highest initiator concentration of 5% (w/w). The minimisation of spatial variations in the SDR films, made possible by the good levels of transverse mixing across the thickness of the film arising from the turbulence eddies [23] is deemed to be responsible for this effect. Also, since the films are much thinner on the SDR (in the range 120–200 μm for the operating conditions used this study), the percentage intensity of UV light penetrating through the whole film should be higher, in accordance with Fig. 7, resulting in not only a higher but also a more uniform rate of radical generation and hence rate of polymerisation. It should be noted that the difficulty in achieving a continuous static film without any breakages due to the surface tension of the fluid at film thickness lower than 400 μm meant that we could not use static film thicknesses in the range generated in the SDR. In spite of this limitation for direct data comparison, the SDR has been shown to have the potential to be more efficient in receiving and transmitting photons than the static film.

The negligible difference between the *initial* rates of polymerisation in the SDR and in the static film at lower initiator concentrations (Fig. 8b) is indicative of oxygen inhibition in the SDR films in the initial stages of the polymerisation. Although all efforts were made to eliminate all oxygen in the SDR environment by purging with nitrogen prior to and during the polymerisation on the disc, there may have still been traces of it in the unsealed reactor system and the possibility of a small degree of oxygen inhibition cannot be ruled out. This inhibitory effect will be accentuated by the thinner films through which the oxygen remnants can diffuse more rapidly and by the lower initiator concentrations.

The so-called gel (autoacceleration) effect is likely to occur in the mixing-deprived static film later on in the polymerisation process, whereby an increase in the rate of reaction and, therefore monomer conversion, in the static film would be observed due to increased viscosity and reduced diffusion ability of the polymer chains. Such a situation leads to a lack of control of the polymerisation process and is best avoided in practice. There is ample evidence from previous studies in different types of reactor configurations [24–26] including the SDR [7,27], to show that efficient mixing can minimise, if not eliminate, the occurrence of a gel effect.

Another characteristic worthy of comment is the shape of each of the plots. The gradients of the static film plots all tend to decrease with time, indicating a decreasing rate (excluding the points at which a secondary rate increase is occurring in accordance with a double gel effect [28] in Fig. 8a and b). This may either be a result of monomer concentration being depleted with time, or, alternatively, of reduced initiator efficiency, arising as a result of the cage effect. On analysis of the SDR plots, however, there is no evidence to suggest that reaction rate decreases with time, even after time intervals comparable with those in the static film. This disproves the hypothesis that observed decreases in rate within the static film in the early stages of the process (i.e. the first 5 s or so) arise as a result of the depleting monomer concentration. If this was the case, then it would also be apparent for the SDR results. We suggest, instead, that the difference observed relates, in all likelihood, to initiator efficiency remaining constant on the SDR due to a suppression of the so-called 'cage effect' of the initiator radicals. Two factors may be responsible for this: (1) the high shear generated in the film under the centrifugal acceleration maintaining a lower effective viscosity in the polymerising mixture than in the static film and (2) intense micromixing within the film increasing the mobility and accessibility of the primary radicals.

3.2.2. Molecular weights

The highest molecular weight generated in the static film (M_n = 21,826 g/mol) is greater than that obtained in the SDR (M_n = 17,873 g/mol). Moreover, the mean value of PDI in the SDR (1.67) is lower than that in the static film (1.88) and the corresponding range of PDI values is narrower on the disc (1.51 < PDI < 1.82) than in the static film (1.65 < PDI < 2.08). The higher molecular weights and broader MWDs attained in the static film are consistent with the proposed reduction in diffusion abilities of the active chains in the increasingly viscous reaction medium. In contrast, with its high shear rates and intense levels of mixing, it is our view that the SDR enables little or no reduction in diffusion abilities.

3.2.3. Copolymer composition

The copolymer composition distributions (CCD) in the SDR and static film are compared against the predicted monodisperse distribution indicated by the green solid line in Fig. 9. The instantaneous mole fraction of butyl acrylate incorporated into the copolymer in our experiments is less than the predicted value of 0.47. The difference in temperatures and reactivity ratios between our work at 348 K and the literature at 343 K [28] may account for this discrepancy.

It is evident that that the CCD within the static film system, which is analogous to a batch system, is rather significant, with the mole fraction of butyl acrylate in the product shifting from 0.45

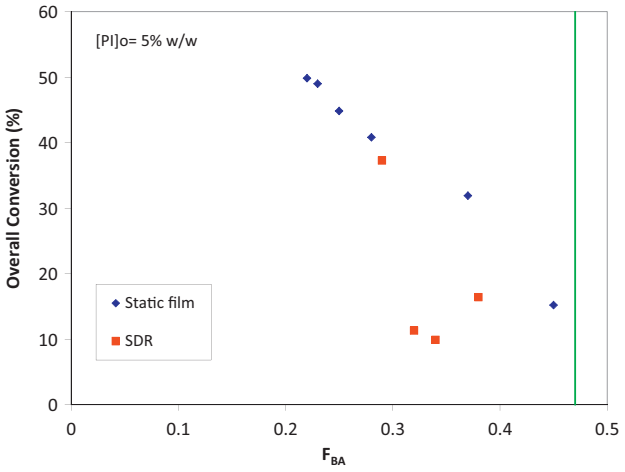

Fig. 9. Copolymer composition distribution in the static film and the SDR (green solid line denotes copolymer composition using reactivity ratios of r_{BA} = 3.07 and r_{VAc} = 0.06 at 343 K [28]). (For interpretation of the references to colour in this figure legend, the reader is referred to the web version of this article.)

at low conversion to 0.2 at higher conversion. A similar behaviour is observed in the SDR. The changes in final copolymer composition in both systems track the evolution in remaining monomer concentration in mixture. It is widely published that good mixing in an ideal CSTR will result in a homogeneous copolymer product, having a monodisperse distribution throughout the course of the polymerisation [29–33]. The SDR, however, exhibits near plug–flow behaviour [23], with excellent mixing in the axial direction (i.e. through the film thickness at a given radial position) but no mixing in the radial direction. Thus, fresh feed introduced at the centre of the disc is not able to effectively mix with the polymer product further along on the disc in order to restore the balance in the composition of the polymerising mixture. The SDR is therefore not equipped to compensate for copolymer compositional drift.

3.3. SDR photo co-polymerisation: theoretical considerations

3.3.1. Light absorption per disc pass

An understanding of the SDR experimental results presented in the preceding sections relies on a quantitative estimation of the efficiency of UV light absorption by the initiator moieties in the flowing film under the various operating conditions studied.

The light absorbed across the whole disc surface per disc pass is given as:

$$I_{a,disc} = \bar{I}_a \cdot 10 \cdot A_{disc} \cdot t_{res} \quad (9)$$

(Note the factor 10 is used to convert the units of $\bar{I}_a$ from mol 10^{-3} cm^{-2} s^{-1} to mol m^{-2} s^{-1}).

where

$$\bar{I}_a = I_0(1 - e^{-\alpha l \bar{C}}) \quad [3, 22] \quad (10)$$

$$I_0 \ (\text{mols photons} \cdot 10^{-3} \text{cm}^{-2}\,\text{s}^{-1}) = \frac{I_0 \ (\text{mW/cm}^2) \cdot \lambda}{h \cdot c \cdot N_A} \quad [3] \quad (11)$$

$$\bar{C} = [\text{PI}]_0 e^{\varphi_i \alpha I_0 t} \quad [22] \quad (12)$$

Fig. 10 highlights how the light absorbed in one disc pass varies with the operating conditions of disc speed, UV intensity and initial photoinitiator concentration. It is clearly observed that UV intensity and photoinitiator concentration have a significant influence on the amount of light absorbed on the disc. The highest absorption is achieved at the highest UV intensity of 106 mW/cm^2 and the highest photo-initiator concentration of 5% (w/w). These effects

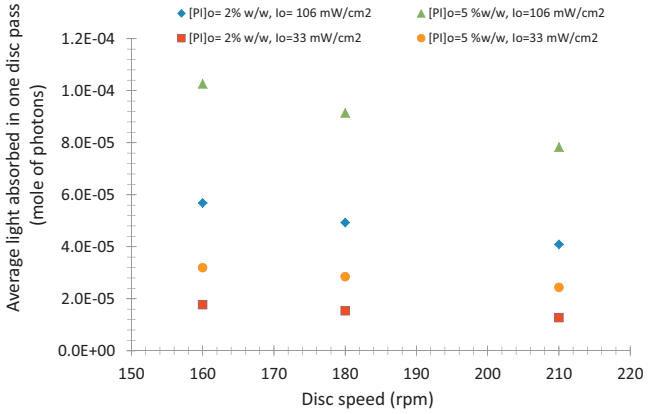

Fig. 10. Effect of disc speed, UV intensity, and initial photoinitiator concentration on light absorption in one disc pass (with constant flowrate of 1.25 ml/s).

are indeed predictable from Eq. (10). Higher mean residence times at lower disc speeds allow longer exposure of the photoinitiator molecules to the UV light, so that more of them can absorb the incident light for their dissociation, according to Eq. (12). These trends are in agreement with the experimental results (Fig. 3) discussed above. Interestingly, the detrimental effects of increased film thickness at the lower disc speeds on light absorption seem to be easily overcome by the increased residence times, presumably because the increases are not significant enough to have an impact.

3.3.2. Efficiency of initiator decomposition

The considerations of light energy available can be extended to include the decomposition efficiency of the initiator, assuming that 1 mol of photons from the UV light source is used to decompose 1 mol of initiator molecules. Here, the number of moles of initiator molecules available in one disc pass, $[\text{PI}]_{disc}$, is estimated as:

$$[\text{PI}]_{disc} = \frac{[\text{PI}]_0}{M_{DMPA}} \cdot \rho_{monomers} \cdot 10^3 \cdot Q \cdot t_{res} \quad (13)$$

Initiator decomposition efficiency can be defined as:

$$\text{Efficiency} = \frac{\text{Available light energy in one disc pass, } I_{a,disc}}{\text{Initiator molecules present on disc, } [\text{PI}]_{disc}} \times 100 \quad (14)$$

A comparison of the effects of flowrate and initiator concentration on light absorbed in one disc pass and the corresponding initiator decomposition efficiency is depicted in Fig. 11. Decomposition

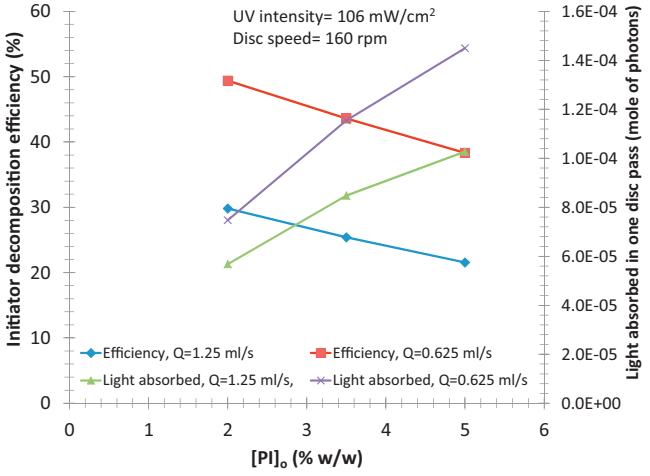

Fig. 11. Comparison of influences of flowrate and initiator concentration on efficiency of decomposition and light absorbed.

efficiency falls as initiator concentration increases (at constant flowrate, disc speed and UV intensity), indicating that, although light absorption increases, there is overall insufficient energy to impart in one pass of the disc for significant decomposition of the majority of the initiator molecules. It is possible to address this limitation by reducing the flowrate Q of the feed, which will cause fewer overall photoinitiator molecules to be present on the disc at any one time. The latter effect is indeed observed to be beneficial in increasing both the decomposition efficiency and the light absorption at any initiator concentration. This beneficial effect of flowrate reduction has been demonstrated experimentally in this study (Fig. 5a).

4. Conclusions

We have demonstrated the feasibility of employing the SDR for the bulk photo-copolymerisation of vinyl acetate with butyl acrylate. A maximum conversion of 37% was achieved in one disc pass, corresponding to a residence time of about 5 s, at a feed flowrate of 0.625 ml/s, disc speed of 160 rpm with the highest UV intensity of 106 mW/cm^2 and highest initiator concentration of 5% (w/w). Disc speed, co-monomer/initiator flowrate, photo-initiator concentration and UV intensity have all been shown to be significant variables which affect the overall monomer conversion and the molecular weight of the polymer. Disc residence time has been found to be a limiting factor in attaining high conversions.

In comparison with the static film, higher overall rates of copolymerisation have been observed in the SDR. The SDR's ability to generate and maintain thinner films which favour a higher and uniform radical generation rate together with the absence of the initiator cage effect may be responsible for this rate enhancement. Copolymer composition drift cannot be addressed in the SDR due its plug–flow characteristics.

Our experimental conversion data in the SDR have been corroborated by a theoretical analysis focused on the effect of light absorption and initiator decomposition efficiency on the disc surface. It is shown that the largest amount of light is absorbed in one disc pass under hydrodynamic conditions in the SDR that give rise to longest UV exposure times, which also correspond to highest overall conversion in the experimental results. Higher UV-intensities and higher initial photo-initiator concentration are also beneficial in this respect. It was shown that the efficiency of initiator decomposition and therefore monomer conversion could be optimised by reducing the flowrate of the feed stream, without any additional energy input.

With its ability to produce thin, controllable and highly mixed films in continuous flow, even on scale-up, the SDR offers much scope for exploiting the relatively untapped possibilities presented by photochemistry applications in general. The potentials for significant energy saving offered by the SDR, which have been reported recently for a thermal polymerisation process [34], in combination with the benefits of UV processing, can provide a realistic energy-efficient solution for many processes.

Acknowledgement

We gratefully acknowledge the Engineering and Physical Science Research Council (EPSRC) for funding this project through a Doctoral Training Award to Christopher Dobie.

References

[1] H.Y. Erbil, Vinyl Acetate Emulsion Polymerization and Copolymerization with Acrylic Monomers, CRC Press, Florida, 2000.
[2] R. Jovanovic, M.A. Dube, Off-line monitoring of butyl acrylate and vinyl acetate homopolymerisation and copolymerisation in toluene, Journal of Applied Polymer Science 82 (2001) 2958–2977.
[3] G. Odian, Principles of Polymerisation, 4th ed., Wiley, New York, 2004.
[4] G.R. Meira, C.V. Luciani, D.A. Estenoz, Continuous bulk process for the production of high-impact polystyrene: recent developments in modeling and control, Macromolecular Reaction Engineering 1 (2007) 25–39.
[5] D. Ruckert, G. Geuskens, Surface modification of polymers—IV. Grafting of acrylamide via an unexpected mechanism using a water soluble photoinitiator, European Polymer Journal 32 (2) (1996) 201–208.
[6] D. Ruckert, G. Geuskens, P. Fondu, S. van Erum, Surface modification of polymers—III. Photoinitiated grafting of water soluble vinyl monomers and influence on fibrinogen adsorption, European Polymer Journal 31 (5) (1995) 431–435.
[7] K. Matyjaszewski, T.P. Davis, Handbook of Radical Polymerisation, Wiley, New York, 2002.
[8] G.A. Miller, L. Gou, V. Narayanan, A.B. Scranton, Modeling of photobleaching for the photoinitiation of thick polymerization systems, Journal of Polymer Science Part A: Polymer Chemistry 40 (2002) 793–808.
[9] G. Oster, N.-L. Yang, Photopolymerization of vinyl monomers, Chemical Reviews 68 (2) (1968) 125–151.
[10] M. Oelgemöller, Highlights of photochemical reactions in microflow reactors, Chemical Engineering and Technology 35 (7) (2012) 1144–1152.
[11] I. Dunkin, Photochemistry, in: J. Clark, D.J. Macquarrie (Eds.), Handbook of Green Chemistry and Technology, Blackwell Sciences, Oxford, 2002, pp. 416–432.
[12] S. Brosillon, L. L'homme, D. Wolbert, Modelling of a falling thin film deposited photocatalytic step reactor for water purification: pesticide treatment, Chemical Engineering Journal 169 (2011) 216–225.
[13] R.J. Braham, T. Andrew, Review of major design and scale-up considerations for solar photocatalytic reactors, Industrial and Engineering Chemistry Research 48 (2009) 8890–8905.
[14] R.J. Jachuck, V. Nekkanti, Continuous photopolymerization of n-butyl acrylate using a narrow channel reactor, Macromolecules 41 (9) (2008) 3053–3062.
[15] K.V.K. Boodhoo, W.A.E. Dunk, R.J. Jachuck, Continuous photo-polymerisation in a novel thin film spinning disc reactor, in: J.V. Crivello, K.D. Belfield (Eds.), Photoinitiated Polymerisation, ACS Symposium Series 847, American Chemical Society, Washington, DC, 2003, pp. 437–450.
[16] S.D. Pask, O. Nuyken, Z.Z. Cai, The spinning disk reactor: an example of a process intensification technology for polymers and particles, Polymer Chemistry 3 (2012) 2698–2707.
[17] S. Beuermann, M. Buback, Rate coefficients of free-radical polymerisation deduced from pulsed laser experiments, Progress in Polymer Science 27 (2002) 191–254.
[18] K.V.K. Boodhoo, W.A.E. Dunk, M. Vicevic, R.J. Jachuck, V. Sage, D.J. Macquarrie, J.H. Clark, Classical cationic polymerization of styrene in a spinning disc reactor using silica-supported BF_3 catalyst, Journal of Applied Polymer Science 101 (1) (2006) 8–19.
[19] J.M. Coulson, J.F. Richardson, Chemical Engineering, vol. 1, 6th ed., Butterworth-Heinemann, Oxford, 2004.
[20] M. Vicevic, K.V.K. Boodhoo, K. Scott, Catalytic isomerisation of alpha-pinene oxide to campholenic aldehyde using silica supported zinc triflate catalysts: II. Performance of immobilised catalysts in a continuous spinning disc reactor, Chemical Engineering Journal 133 (1–3) (2007) 43–57.
[21] K.V.K. Boodhoo, W.A.E. Dunk, R.J. Jachuck, Influence of centrifugal field on free-radical polymerization kinetics, Journal of Applied Polymer Science 85 (11) (2002) 2283–2286.
[22] K.V.K. Boodhoo, W.A.E. Dunk, M.S. Jassim, R.J. Jachuck, Thin film solvent-free photopolymerization of n-butyl acrylate. I. Static film studies, Journal of Applied Polymer Science 91 (4) (2004) 2079–2095.
[23] S. Mohammadi, K.V.K. Boodhoo, Online conductivity measurement of residence time distribution of thin film flow in the spinning disc reactor, Chemical Engineering Journal 207–208 (2012) 885–894.
[24] E.J. Troelstra, L.L. van Dierendonck, L.P.B. Janssen, A. Renken, Modeling of a BUS-Kneader as a polymerisation reactor for acrylates. Part II. Methyl methacrylate based resins, Polymer Engineering and Science 42 (1) (2002) 240–247.
[25] M. Cioffi, A.C. Hoffman, L.P.B.M. Janssen, Instabilities in free-radical polymerisation, Nonlinear Analysis 47 (2001) 897–906.
[26] M. Cioffi, K.J. Ganzeveld, A.C. Hoffmann, L.P.B.M. Janssen, A rheokinetic study of bulk free-radical polymerisation performed with a helical barrel rheometer, Polymer Engineering and Science 44 (2004) 179–185.
[27] K.V.K. Boodhoo, R.J. Jachuck, Process intensification: spinning disc reactor for styrene polymerisation, Applied Thermal Engineering 20 (12) (2000) 1127–1146.
[28] M. Dube, A. Penlidis, A systematic approach to the study of multicomponent polymerisation kinetics—the butyl acrylate/methyl methacrylate/vinyl acetate example: 1. Bulk copolymerisation, Polymer 36 (1995) 587–598.
[29] K.F. O'Driscoll, R. Knorr, Multicomponent polymerisation. II. The effect of mixing on copolymerisation in continuous stirred tank reactors, Macromolecules 2 (1969) 507.
[30] S. Belkhiria, T. Meyer, A. Renken, A study of micromixing in polymerisation reactions and its application in experimental copolymerisation, Industrial Mixing Technology, AIChE Symposium Series 90 (1994) 117–122.

[31] P. Fleury, Bulk polymerisation or copolymerisation in a novel continuous Kneader reactor, Macromolecular Symposium 243 (2006) 287–298.
[32] C. Sayer, R. Giudici, Simulation of emulsion copolymerization reactions in a continuous pulsed sieve-plate column reactor, Brazilian Journal of Chemical Engineering 21 (3) (2004) 459–470.
[33] C.A. Scholtens, J. Meuldijk, A.A.H. Drinkenburg, Production of copolymers with a predefined intermolecular chemical composition distribution by emulsion polymerisation in a continuously operated reactor, Chemical Engineering Science 56 (3) (2001) 955–962.
[34] D. Ghiasy, K.V.K. Boodhoo, Opportunities for energy saving by intensified process technologies in the chemical and processing industries, in: K.V.K. Boodhoo, A.P. Harvey (Eds.), Process Intensification for Green Chemistry: Engineering Solutions for Sustainable Chemical Processing, Wiley-Blackwell, Oxford, 2013, pp. 379–392.
[35] M.D. Goodner, C.N. Bowman, in: T.E. Long, M.O. Hunt (Eds.), Solvent-Free Polymerizations and Processes. Minimization of Conventional Organic Solvents, ACS Symposium Series 713, American Chemical Society, Washington, DC, 1998.